Research Article

Electronic and Thermal Transport Properties of Complex Structured Cu-Bi-Se Thermoelectric Compound with Low Lattice Thermal Conductivity

Jae-Yeol Hwang,[1] Hyeona Mun,[2] Jung Young Cho,[3] Sang Sun Yang,[4] Kyu Hyoung Lee,[3] and Sung Wng Kim[1,2]

[1] *Center for Integrated Nanostructure Physics, Institute for Basic Science (IBS), Daejeon 305-701, Republic of Korea*

[2] *Department of Energy Science, Department of Physics, Sungkyunkwan University, Suwon 440-746, Republic of Korea*

[3] *Materials R&D Center, Samsung Advanced Institute of Technology, Samsung Electronics, Yongin 446-712, Republic of Korea*

[4] *Powder and Ceramics Division, Powder Technology Department, Korea Institute of Materials Science, Changwon 642-831, Republic of Korea*

Correspondence should be addressed to Kyu Hyoung Lee; kyuhyoung.lee@samsung.com
and Sung Wng Kim; kimsungwng@skku.edu

Received 22 June 2013; Revised 20 July 2013; Accepted 5 August 2013

Academic Editor: Hyung-Ho Park

Monoclinic $Cu_{x+y}Bi_{5-y}Se_8$ structure has multiple disorders, such as randomly distributed substitutional and interstitial disorders by Cu as well as asymmetrical disorders by Se. Herein, we report the correlation of electronic and thermal properties with the structural complexities of $Cu_{x+y}Bi_{5-y}Se_8$. It is found that the interstitial Cu site plays an important role not only to increase the electrical conductivity due to the generation of electron carriers but also to reduce the thermal conductivity mainly due to the phonon scattering by mass fluctuation. With impurity doping at the interstitial Cu site, an extremely low lattice thermal conductivity of 0.32 W·m^{-1}·K^{-1} was achieved at 560 K. These synergetic effects result in the enhanced dimensionless figure of merit (ZT).

1. Introduction

In thermoelectric (TE) materials, thermal energy is directly converted into electrical energy and vice versa through the flow of charge carriers (electrons or holes) in solid state without any moving parts [1, 2]. The performance of TE device depends on the temperature gradient (ΔT) and the dimensionless figure of merit (ZT) in TE material. The conversion efficiency of TE material is governed by ZT, which is defined as $ZT = S^2 \cdot \sigma \cdot T/\kappa$, where S is the thermopower (Seebeck coefficient), σ is the electrical conductivity, κ is the thermal conductivity, and T is the absolute temperature. Intuitively, good TE materials should have sufficiently large S, high σ, and low κ. Based on this relation, there are two different kinds of straightforward strategies for achieving high ZT. The first one is maximizing power factor (PF = $S^2 \cdot \sigma$) by the modification of the electronic states through the optimization of doping, introduction of nanoscale materials, and

so forth. The other one is minimizing κ by the perturbation of structural arrangements for enhancing phonon scattering through solid-solution alloying [3–6], nanostructuring [7, 8], and the development of new materials with intrinsically low κ. However, since σ, S, and κ are the functions of charge carriers as well as these physical parameters are intercorrelated to each other, it is very difficult to control these parameters individually. Recent TE researches have been mainly focused on breaking the trade-off relationship between σ and κ by reducing the lattice thermal conductivity (κ_{latt}) due to the relative easiness of reducing κ_{latt} without considerably affecting other electronic transport parameters (S and σ). Thus, extensive researches have been focused on reducing κ_{latt} by utilizing nanostructures and compositional inhomogeneities of state-of-the-art TE materials such as Bi_2Te_3, PbTe, and SiGe [3–8]. It has been reported that dramatically reduced κ_{latt} in TE materials is due to one of

the following mechanisms: alloy scattering [3–6], resonant scattering [9–13], anharmonic scattering [14], and interface scattering of phonons [15–17] or their combination.

Recently, much effort has been focused on discovering new semiconducting materials with intrinsically low κ_{latt}. Such materials have a solid potential compared to conventional TE materials because their κ_{latt} can be further reduced by compositional and microstructural engineering without sacrificing the other electronic properties. The common structural characteristics of low κ_{latt} materials are complex structures, which have relatively large unit cells, sublattice disorders, low crystal symmetry, and/or a variety of atom types combined with random distributions. These result in the effective phonon scatterings, which make these materials promising candidates for TE applications.

By understanding the origin of low κ in complex structured system, it is possible to find a clue for novel TE materials with an appropriate structure and to manipulate structural arrangement for the achievement of low κ in conventional TE materials. In a previous article [18], we reported new TE materials, which are the pavonite homologues $Cu_{x+y}Bi_{5-y}Se_8$ ($1.2 \leq x \leq 1.5$, $0.1 \leq y \leq 0.4$) with low κ_{latt} (0.41–0.55 $W \cdot m^{-1} \cdot K^{-1}$ at 300 K) owing to the structural complexity. In the present study, we investigated the electronic and thermal transport properties in the view point of the correlation with crystal structure in order to clarify the origin of TE properties in the homologous $Cu_{x+y}Bi_{5-y}Se_8$ compounds.

2. Experimental

Crystal ingots of $Cu_{x+y}Bi_{5-y}Se_8$ compounds were fabricated by conventional melting technique by the use of high-purity elemental Cu (99.999%, CERAC), Bi (99.999%, 5N Plus), and Se (99.9%, 5N Plus) as starting materials. The stoichiometric mixtures of the elements were loaded into a quartz tube of 14 mm in diameter. The tube was vacuum-sealed and the mixed contents were melted in a furnace for 10 hrs at 1273 K; then, they were water quenched. The ingots were ground using ball mill, and compacted bulk samples of 10 mm in diameter and 13 mm in thickness were prepared using spark plasma sintering (SPS) technique under dynamic vacuum and with the application of 50 MPa of uniaxial pressure at 663 K. The relative densities of the resulting consolidated samples were found to range from 7.22 to 7.48 $g \cdot cm^{-3}$, which are more than 95% of the theoretical value. We used $Cu_{1.7}Bi_{4.7}Se_8$ ($Cu_{x+y}Bi_{5-y}Se_8$, $x = 1.4$, $y = 0.3$) as a reference material, and small amount (w and $z = 0.0085$ and 0.025 for the interstitial and substitutional M sites, resp.) of Zn or In was introduced in host $Cu_{1.7-w}M_wBi_{4.7}Se_8$ or $Cu_{1.7}Bi_{4.7-z}M_zSe_8$ matrix to elucidate the electronic and thermal properties according to the different carrier concentrations. The electronic transport properties including σ and S were measured from 300 K to 560 K using an ULVAC ZEM-3 system. The κ values ($\kappa = \rho_s \cdot C_p \cdot \lambda$) were calculated from measurements taken separately: sample density (ρ_s), heat capacity (C_p), and thermal diffusivity (λ) measured under vacuum by laser-flash method (TC-9000, ULVAC, Japan), in which C_p was used as the constant value
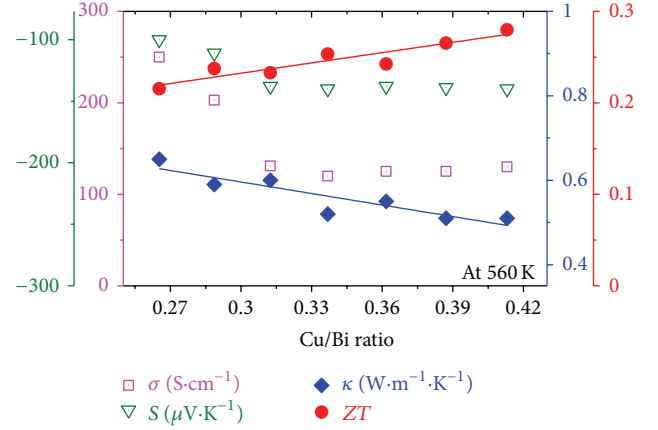

Figure 1: Electrical conductivity (σ), Seebeck coefficient (S), thermal conductivity (κ), and ZT as functions of Cu/Bi ratio in $Cu_{x+y}Bi_{5-y}Se_8$ ($1.2 \leq x \leq 1.5$, $0.1 \leq y \leq 0.4$) pavonite homologues. All data were acquired at 560 K.

of 0.225 $J \cdot g^{-1} \cdot K^{-1}$ estimated from the Dulong-Petit fitting using low temperature C_p data. All measured data, which were acquired at the same dimension and configuration, are obtained within the experimental error of about 5%.

3. Results and Discussions

Figure 1 shows TE properties for the homologous $Cu_{x+y}Bi_{5-y}Se_8$ ($1.2 \leq x \leq 1.5$, $0.1 \leq y \leq 0.4$) system at 560 K with varying compositional ratio between Cu and Bi. The absolute value of S decreases linearly with increasing σ, indicating that the semiconducting transport properties do not significantly change with varying the Cu/Bi ratio. Based on theoretical calculations of the previous report, interstitial Cu is regarded as the main source of electron carriers in the $Cu_{x+y}Bi_{5-y}Se_8$ system [18]. Because the electron distributions around interstitial Cu ions, which are shown in the crystal structure of Cu-Bi-Se pavonite compound (Figure 2(a)), overlapped each other along b-axis, the degree of overlapping depends on the content of the interstitial Cu. This might be a possible reason for the changes in electrical properties by perturbing Cu sites, since the interstitial Cu sites locate along b-axis and work as an electrical conduction path, leading to an improvement of electron transfer across the basal plane. On the other hand, κ decreases from 0.65 to 0.51 $W \cdot m^{-1} \cdot K^{-1}$ by increasing Cu content. The highest ZT value of 0.27 at 560 K was obtained in the $Cu_{1.9}Bi_{4.6}Se_8$ composition, which has the highest Cu concentration among samples, mainly due to its low κ. Thus, it is suggested that statistically distributed interstitial Cu along b-axis may be the main factor affecting the electronic (by generating electron carriers) and thermal transport (by enhancing phonon scattering) properties in this system. In order to understand the TE transport behavior based on the roles of the interstitial Cu and substitutional Bi sites, we individually modified those sites by impurity doping.

$Cu_{1.7}Bi_{4.7}Se_8$ was chosen as a base composition for doping, since this composition showed stable structure

(a)

(b)
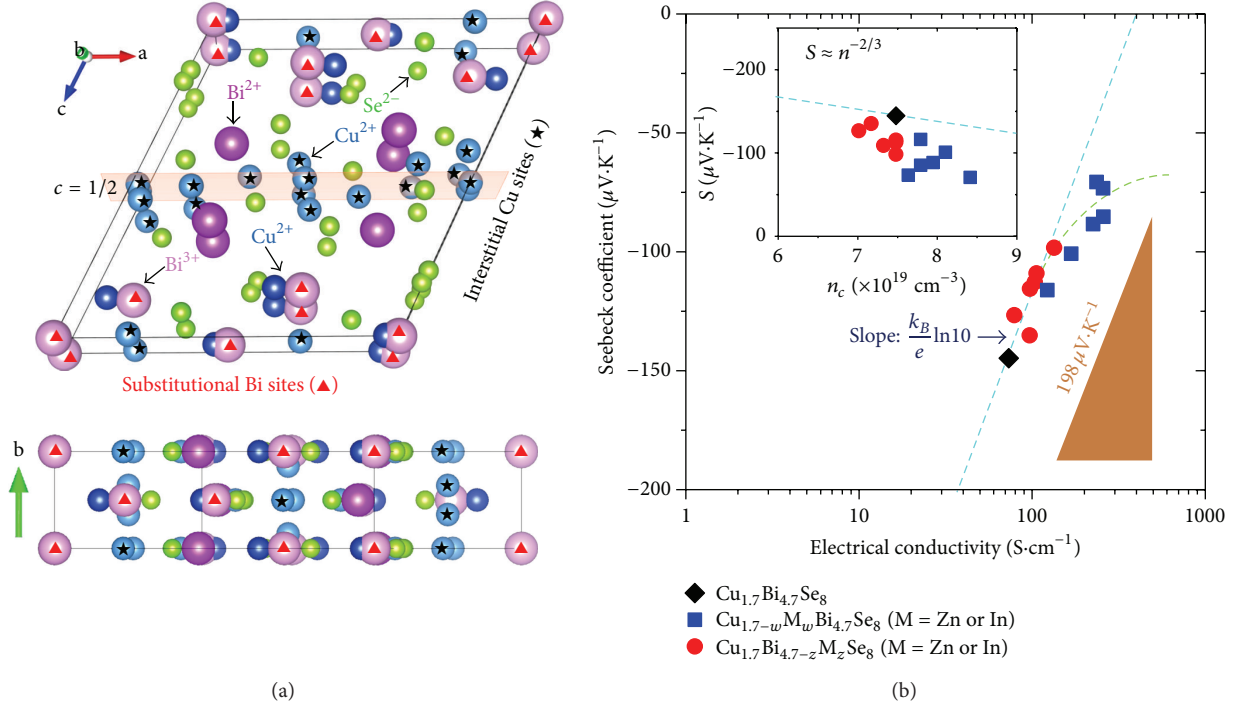
FIGURE 2: (a) Crystal structure of $Cu_{1.7}Bi_{4.7}Se_8$ with interstitial Cu and substitutional Bi sites. (b) Seebeck coefficient as a function of electrical conductivity (σ) for Cu-Bi-Se system. Blue and red dots indicate $Cu_{1.7-w}M_wBi_{4.7}Se_8$ and $Cu_{1.7}Bi_{4.7-z}M_zSe_8$ systems, respectively. Black dot is a base $Cu_{1.7}Bi_{4.7}Se_8$ compound. The inset is Pisarenko plot at 300 K, representing the Seebeck coefficient (S) as a function of carrier concentration (n_c). The dashed line corresponds to the theoretically expected curve for $Cu_{1.7}Bi_{4.7}Se_8$ with effective mass of $m^* \sim 0.21m_0$.

and reproducible physical properties. Figure 2(b) shows the Jonker plot of Cu-Bi-Se system. Most of the experimental data points for $Cu_{1.7}Bi_{4.7-z}M_zSe_8$ compounds lie on the straight line (cyan dashed) with the slope of $198\,\mu V\cdot K^{-1}$. However, in case of the interstitial Cu site modified $Cu_{1.7-w}M_wBi_{4.7}Se_8$ compounds, the slope (green dashed line) was changed in the region of largely increased σ (Figure 2(b)), indicating that the electronic state was altered to a highly degenerate state by doping at the interstitial Cu sites. In Pisarenko plot (the inset of Figure 2(b)), all data points lie below the theoretically expected Pisarenko curve (cyan) for undoped $Cu_{1.7}Bi_{4.7}Se_8$ with effective mass of m^* ($\sim0.21m_0$). These electronic transport properties might be related to the changes in the Hall mobility (μ_H) and m^* of doped compounds. In order to clarify the origin for affecting S in doped compounds, m^* values were calculated using the measured S and the carrier concentration (n_c) for the whole samples. The m^* is one of the critical factors determining S and estimated with the following equation:

$$m^* = \frac{h^2}{2k_BT}\left[\frac{n_c}{4\pi F_{1/2}(\eta)}\right]^{2/3}, \quad (1)$$

where h, k_B, F_n, and η are the Planck constant, Boltzmann constant, nth order Fermi integral, and the reduced Fermi energy, respectively.

As shown in Figure 3, m^* was decreased by the doping compared to that of undoped compound. It should be noted that m^* values of the interstitial Cu site modified
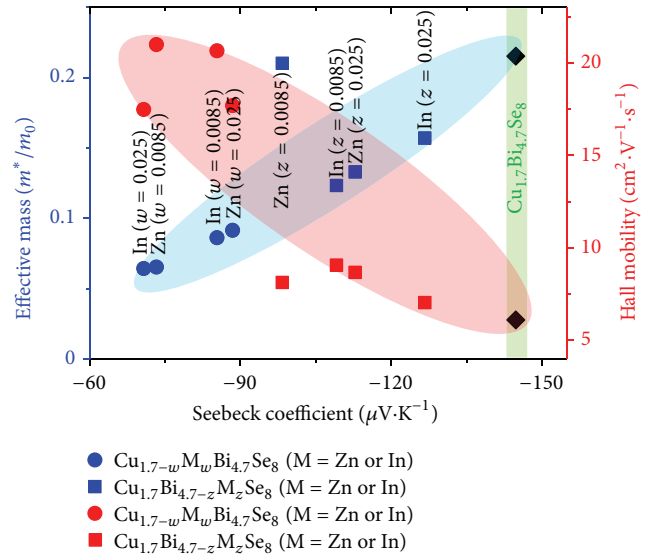

FIGURE 3: Effective mass (m^*/m_0) and Hall mobility (μ_H) as functions of Seebeck coefficient (S) for $Cu_{1.7-w}M_wBi_{4.7}Se_8$ and $Cu_{1.7}Bi_{4.7-z}M_zSe_8$ with varying doping levels and dopants.

$Cu_{1.7-w}M_wBi_{4.7}Se_8$ compounds were much lower than those of $Cu_{1.7}Bi_{4.7-z}M_zSe_8$. Furthermore, μ_H was inversely proportional to m^* due to the reduced mass. In principle, the reduced m^* enables the energetic movement of charge carriers in the highly degenerate semiconductors, resulting
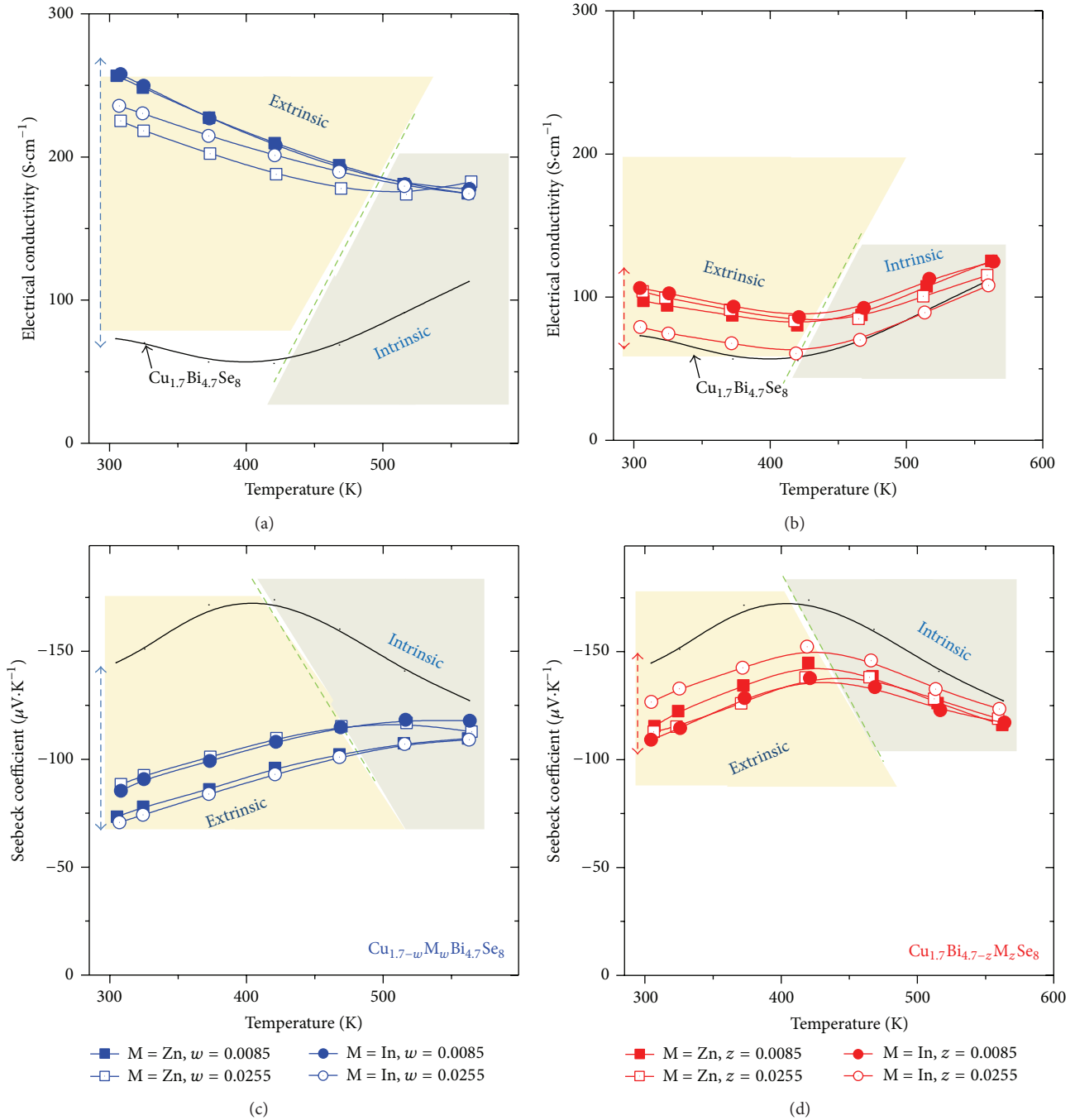
(a)

(b)

(c)

(d)

FIGURE 4: Electrical conductivity (σ) as a function of temperature for (a) $Cu_{1.7-w}M_wBi_{4.7}Se_8$ and (b) $Cu_{1.7}Bi_{4.7-z}M_zSe_8$. Seebeck coefficient ($S$) as a function of temperature for (c) $Cu_{1.7-w}M_wBi_{4.7}Se_8$ and (d) $Cu_{1.7}Bi_{4.7-z}M_zSe_8$.

in the decrease of S. Considering the slight change of n_c in the inset of Figure 2(b), it is concluded that the decrease in S is largely affected by the reduced m^* via the modification of interstitial Cu site.

In Figure 4(a), σ of $Cu_{1.7-w}M_wBi_{4.7}Se_8$ was drastically changed by the modification of Cu sites compared to that of Bi sites ($Cu_{1.7}Bi_{4.7-z}M_zSe_8$). According to the theoretical calculation, interstitial Cu generates electron carriers in $Cu_{x+y}Bi_{5-y}Se_8$ system [18]. Therefore, more electrons can be

generated by the elemental doping at the interstitial Cu site. Indeed, higher n_c, μ_H, and the smaller m^* were observed in $Cu_{1.7-w}M_wBi_{4.7}Se_8$ compared to those of $Cu_{1.7}Bi_{4.7-z}M_zSe_8$. In Figures 4(a) and 4(b), with increasing the doping level, the region of intrinsic conduction also shifts to higher temperatures. This is a typical behavior of a degenerate semiconductor, since the increased extrinsic majority carriers suppress the contribution of the minority carriers and hence increase the onset temperature of intrinsic conduction.
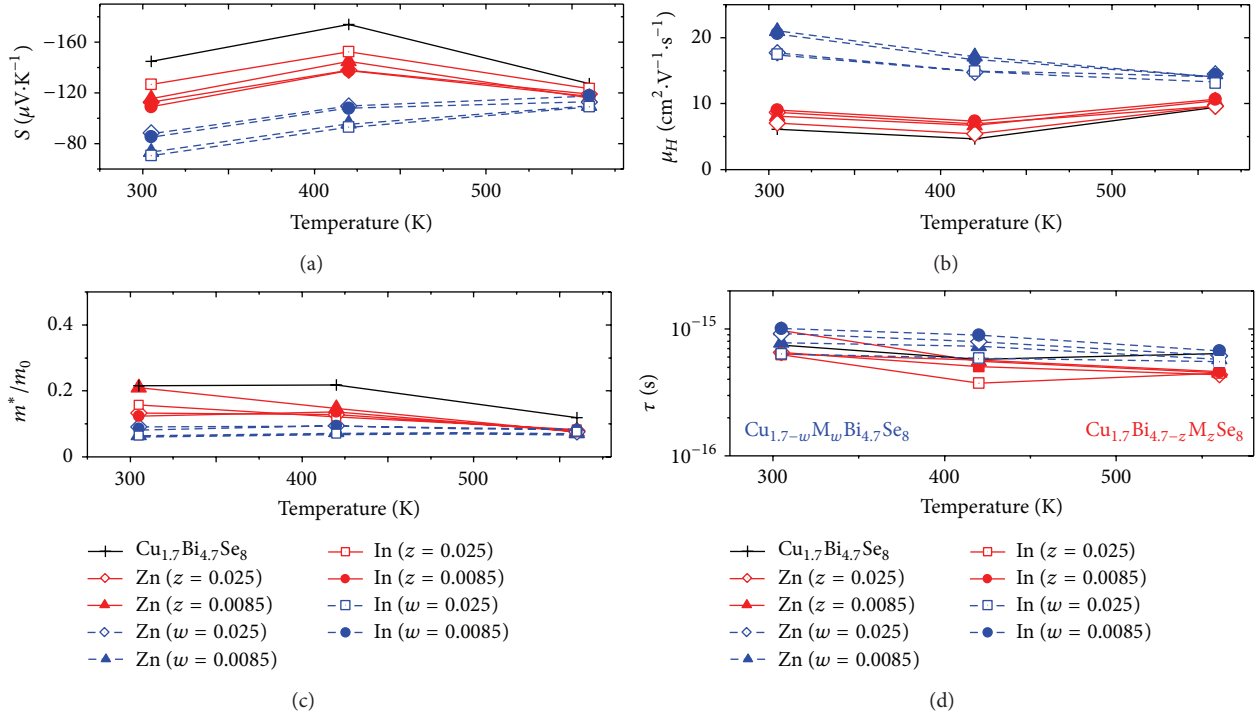
FIGURE 5: (a) Seebeck coefficient (S), (b) Hall mobility (μ_H), (c) effective mass (m^*/m_0), and (d) carrier relaxation time (τ) as a function of temperature for $Cu_{1.7-w}M_wBi_{4.7}Se_8$ and $Cu_{1.7}Bi_{4.7-z}M_zSe_8$ with varying doping levels and dopants.
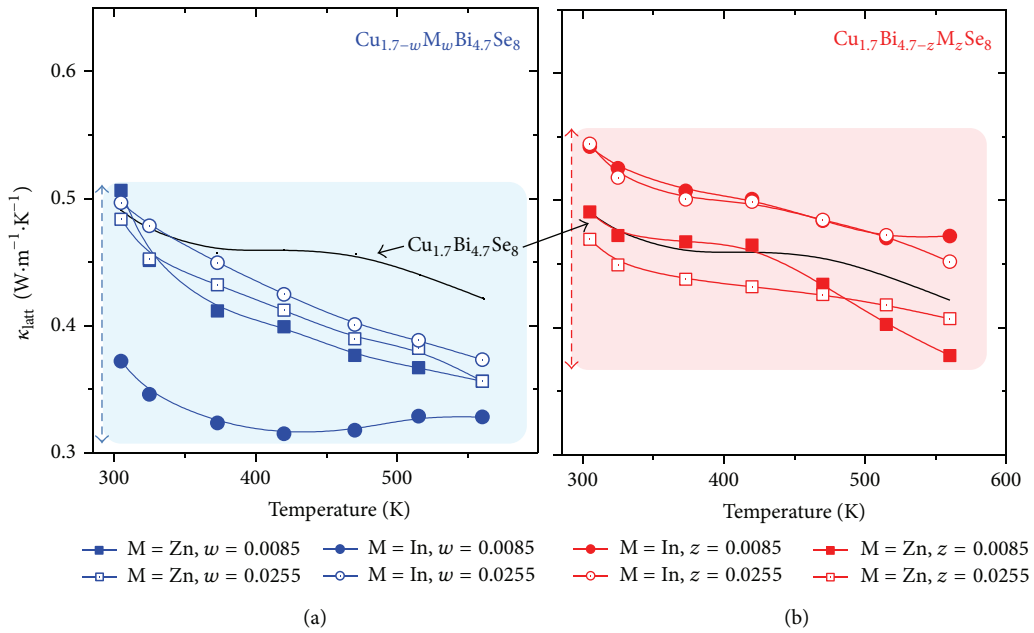

FIGURE 6: Lattice thermal conductivity (κ_{latt}) as a function of temperature for (a) $Cu_{1.7-w}M_wBi_{4.7}Se_8$ and (b) $Cu_{1.7}Bi_{4.7-z}M_zSe_8$ with varying doping levels and dopants.

As shown in Figures 4(c) and 4(d), negative S values for all samples were observed over the entire temperature range, suggesting that the electrical conduction was dominated by n-type carriers. In Figure 5, it was confirmed that the change in S at 560 K was due to the combined effect of decreased m^*

and increased μ_H. Regardless of doping level and sites, carrier relaxation time (τ) was nearly the same (a few *femtoseconds*) for all samples. Figure 6 shows κ_{latt} as a function of temperature. The value of κ_{latt} was calculated from the relation of $\kappa = \kappa_{latt} + \kappa_{elec}$, in which κ_{elec} is the electronic contribution.

The value of κ_{elec} was estimated using the Wiedemann-Franz law, $\kappa_{elec} = L \cdot T \cdot \sigma$, in which L denotes the Lorenz number, taken to be $L = (\pi^2/3)(k_B/e)^2 \sim 2.45 \times 10^{-8}$ $V^2 \cdot K^{-2}$. However, this value is valid for the estimation of κ_{latt} in metals, not in heavily doped semiconductors like TE materials especially at high temperature. In semiconductors, the L depends on η and scattering factor (r), which can be derived from the temperature dependence of μ_H ($\mu_H \propto T^{-(3/2)+r}$) and decreases as η decreases with increasing temperature. The L is given as

$$L = \left(\frac{k_b}{e}\right)^2 \left(\frac{(r + 7/2)\, F_{r+(5/2)}\,(\eta)}{(r + 3/2)\, F_{r+(1/2)}\,(\eta)} \right.$$
$$\left. - \left[\frac{(r + (5/2))\, F_{r+(3/2)}\,(\eta)}{(r + (3/2))\, F_{r+(1/2)}\,(\eta)} \right]^2 \right), \tag{2}$$

where $F_n(\eta)$ is the nth order Fermi integral, $F_n(\eta) = \int_0^\infty (x^n/(1 + e^{x-\eta}))dx$ [19].

Calculated L was nearly constant in all compounds and was in the range of 2.48–2.58×10^{-8} $V^2 \cdot K^{-2}$. As shown in Figure 6, κ_{latt} was much decreased by the modification of Cu sites compared to that of Bi sites. This is mainly ascribed to the mass difference between site ions (Cu or Bi) and dopants. Indeed, the mass difference for interstitial Cu and In is 114.82 compared to 29.2 for the substitutional Bi and In. The values of κ, ranging from 0.47 $W \cdot m^{-1} \cdot K^{-1}$ to 0.69 $W \cdot m^{-1} \cdot K^{-1}$, were found for all compounds, and κ showed a weak temperature dependence. These κ values are much lower than those of state-of-the-art low κ_{latt} systems, such as Zn_4Sb_3 ($\kappa \sim 1.05$ $W \cdot m^{-1} \cdot K^{-1}$ at 300 K) [20] and $Cu_{2-x}Se$ ($\kappa \sim 1$ $W \cdot m^{-1} \cdot K^{-1}$ at 400 K) [21]. We suggest that the reason of the extremely low κ values in this system is due to the strong phonon scattering and the short phonon mean free path of below 1 nm, which is much shorter than the size of unit cell of this structure. The strong phonon scattering is mainly attributed to the structural complexities based on the combined effect of point defects and intrinsic disorders. The maximum ZT values achieved in this study for Cu site and Bi site modified $Cu_{1.6915}In_{0.0085}Bi_{4.7}Se_8$ and $Cu_{1.7}Bi_{4.6915}Zn_{0.0085}Se_8$ were 0.25 and 0.18 at 560 K, respectively. It is expected from the low σ values of Cu-Bi-Se system that the present TE properties can be much enhanced by optimizing PF through tuning n_c. The modification of Cu site is an effective way to reduce κ_{latt} compared to that of Bi site. It is worth noting that intrinsically low κ of this material is less sensitive to temperature gradient because of the complex mixture of extraordinary structural disorders. There is still remaining a possibility for the further improvement of TE performance by the optimization of resonant level doping to enhance PF without sacrificing κ.

4. Conclusions

The electronic and thermal transport properties of $Cu_{1.7}Bi_{4.7}Se_8$ pavonite homologues ($N = 3$) with monoclinic $C2/m$ space group were investigated in the view point of the correlation with complex crystal structure via the modification of Cu or Bi sites with dopants. σ and κ_{latt} were much affected by the modification of Cu sites compared to that of Bi sites. This is due to the origin of n-type conduction and the intrinsically low κ_{latt}, which is highly related to the structural configuration of the interstitial Cu sites in this system. Though the $Cu_{1.7}Bi_{4.7}Se_8$ compound showed an extremely low κ_{latt}, additional ~30% reduction in κ_{latt} was achieved by the modification of Cu sites. Therefore, we anticipate that the further fine-tuning of the electronic and thermal properties based on the correlated findings about structural modifications gives a possible enhancement of TE performance in the Cu-Bi-Se system.

References

[1] F. J. Disalvo, "Thermoelectric cooling and power generation," *Science*, vol. 285, no. 5428, pp. 703–706, 1999.

[2] G. J. Snyder and E. S. Toberer, "Complex thermoelectric materials," *Nature Materials*, vol. 7, no. 2, pp. 105–114, 2008.

[3] H. J. Goldsmid, "Recent studies of bismuth telluride and its alloys," *Journal of Applied Physics*, vol. 32, no. 10, pp. 2198–2202, 1961.

[4] B. Abeles, "Lattice thermal conductivity of disordered semiconductor alloys at high temperatures," *Physical Review*, vol. 131, no. 5, pp. 1906–1911, 1963.

[5] W. M. Yim, E. V. Fitzke, and F. D. Rosi, "Thermoelectric properties of Bi_2Te_3-Sb_2Te_3-Sb_2Se_3 pseudo-ternary alloys in the temperature range 77 to 300 K," *Journal of Materials Science*, vol. 1, no. 1, pp. 52–65, 1966.

[6] C. Wood, "Materials for thermoelectric energy conversion," *Reports on Progress in Physics*, vol. 51, no. 4, pp. 459–539, 1988.

[7] B. Wölfing, C. Kloc, J. Teubner, and E. Bucher, "High performance thermoelectric Tl_9BiTe_6 with an extremely low thermal conductivity," *Physical Review Letters*, vol. 86, no. 19, pp. 4350–4353, 2001.

[8] K. Kurosaki, A. Kosuga, H. Muta, M. Uno, and S. Yamanaka, "Ag_9TlTe_5: a high-performance thermoelectric bulk material with extremely low thermal conductivity," *Applied Physics Letters*, vol. 87, no. 6, Article ID 061919, 2005.

[9] B. C. Sales, D. Mandrus, and R. K. Williams, "Filled skutterudite antimonides: a new class of thermoelectric materials," *Science*, vol. 272, no. 5266, pp. 1325–1328, 1996.

[10] V. Keppens, D. Mandrus, B. C. Sales et al., "Localized vibrational modes in metallic solids," *Nature*, vol. 395, no. 6705, pp. 876–878, 1998.

[11] J. Yang, W. Zhang, S. Q. Bai, Z. Mei, and L. D. Chen, "Dual-frequency resonant phonon scattering in $Ba_xR_yCo_4Sb_{12}$ ($R =$ La, Ce, and Sr)," *Applied Physics Letters*, vol. 90, no. 19, Article ID 192111, 2007.

[12] J. L. Cohn, G. S. Nolas, V. Fessatidis, T. H. Metcalf, and G. A. Slack, "Glasslike heat conduction in high-mobility crystalline

semiconductors," *Physical Review Letters*, vol. 82, no. 4, pp. 779–782, 1999.

[13] D.-Y. Chung, T. Hogan, P. Brazis et al., "CsBi$_4$Te$_6$: a high-performance thermoelectric material for low- temperature applications," *Science*, vol. 287, no. 5455, pp. 1024–1027, 2000.

[14] O. Delaire, J. Ma, K. Marty et al., "Giant anharmonic phonon scattering in PbTe," *Nature Materials*, vol. 10, no. 8, pp. 614–619, 2011.

[15] W. Xie, X. Tang, Y. Yan, Q. Zhang, and T. M. Tritt, "Unique nanostructures and enhanced thermoelectric performance of melt-spun BiSbTe alloys," *Applied Physics Letters*, vol. 94, no. 10, Article ID 102111, 2009.

[16] W. K. Liebmann and E. A. Miller, "Preparation phase-boundary energies, and thermoelectric properties of Insb-Sb eutectic alloys with ordered microstructures," *Journal of Applied Physics*, vol. 34, no. 9, pp. 2653–2659, 1963.

[17] A. I. Hochbaum, R. Chen, R. D. Delgado et al., "Enhanced thermoelectric performance of rough silicon nanowires," *Nature*, vol. 451, no. 7175, pp. 163–167, 2008.

[18] J. Y. Cho, H. Mun, B. Ryu et al., "Cu-Bi-Se-based pavonite homologue: a promising thermoelectric material with low lattice thermal conductivity," *Journal of Material Chemistry A*, vol. 1, no. 34, pp. 9768–9774, 2013.

[19] L. D. Zhao, S. Hao, S. H. Lo et al., "High thermoelectric performance via hierarchical compositionally alloyed nanostructures," *Journal of the American Chemical Society*, vol. 135, no. 19, pp. 7364–7370, 2013.

[20] G. J. Snyder, M. Christensen, E. Nishibori, T. Caillat, and B. B. Iversen, "Disordered zinc in Zn$_4$Sb$_3$ with phonon-glass and electron-crystal thermoelectric properties," *Nature Materials*, vol. 3, no. 7, pp. 458–463, 2004.

[21] H. Liu, X. Shi, F. Xu et al., "Copper ion liquid-like thermoelectrics," *Nature Materials*, vol. 11, no. 5, pp. 422–425, 2012.